Hydroxyapatite Film Formation by Aerosol Deposition Method †

TSUKAMOTO Masahiro*, FUJIHARA Toshiaki**, ABE Nobuyuki***, MIYAKE Shoji****
KATTO Masahito*****, NAKAYAMA Takeyoshi****** and AKEDO Jun*******

Abstract

A coating technology was developed to form hydroxyapatite (HAp) films on the surface of titanium (Ti) plates with the aerosol deposition method using an ultrafine particle (UFP) beam. The UFP beam was composed of HAp particles of submicron size. The dependence of the film s formation on the beam s incident angle was also investigated. A thick HAp film was produced at an incident angle of 0°, but the film did not display good adhesion to the Ti plate. At incident angles of 40° and 60°, the HAp films formed were fine, although not as thick as that formed at 0°. The adhesion strength between the HAp film and the Ti plate was found to be higher than 20 MPa in the films formed at both 40° and 60°.

KEY WORDS: (Aerosol deposition method), (Ultrafine particle beam), (Hydroxyapatite),(Biomaterial)

1. Introduction

Hydroxyapatite (HAp) has good biocompatibility but is difficult to use as an implant for bone substitution because it has much lower mechanical reliability and workability than such conventional biomaterials as titanium (Ti) and the titanium alloy Ti-6Al-4V [1, 2]. A material that combines the mechanical properties of such metals and the bioactivity of HAp could be used in implants. A coating with strong cohesive strength, good adhesion to the substrate, low porosity, a high degree of crystallinity and high chemical purity is required. Various deposition methods for forming an HAp film on Ti and Ti-based substrates have been reported, including plasma spraying [3], ion-beam sputtering [4], ion-beam assisted deposition [5], and pulsed laser deposition [6]. In addition to these methods, coating technology by the aerosol deposition (AD) method using an ultrafine particle (UFP) beam, based on the gas deposition method (GDM) [7], can also be applied. The UFP beam is composed of submicron-size particles accelerated by gas flows to velocities of 200 - 650 m/s [8]. When a Ti substrate is irradiated with a UFP beam, the HAp particles collide with the substrate and form a film. It is probable that some of the particles kinetic energy is converted during impact into thermal energy that promotes bonding between the particles and substrate. However, the actual bonding mechanism has not yet been elucidated. In the AD method, neither the particles nor the substrate are heated during deposition, which is advantageous compared to other coating methods that require high temperatures (ex. thermal spraying and pulsed laser deposition). For example, the particles can retain their crystal structure during UFP beam irradiation. This technology has already been effectively applied to the formation of lead-zirconate-titanate (PZT) films [9], but there have been no reports on the utilization of this method for

† Received on January 31,2003
* Assistant professor
** Graduate student of Kinki University
*** Associate professor
**** Professor
*****Lecturer of Kinki University
******Professor of Kinki University
*******Group reader of National Institute of Advanced Industrial Science and Technology

Transactions of JWRI is published by Joining and Welding Research Institute of Osaka University, Ibaraki, Osaka 567-0047, Japan

bioceramics such as HAp. The cold spray method is very similar to the AD method [10], but there have been no reports of its use for the successful formation of ceramic coatings on metal substrates.

In the first stage of this study to produce a HAp film on Ti plates with the AD method using a UFP beam, we investigated the effect of varying the UFP beam's incident angle on the surface and thickness of the HAp film produced. The adhesion strength and crystallinity were also evaluated.

2. Experimental Procedures

The AD film fabrication system was primarily composed of an aerosol chamber and a processing chamber connected by a Teflon tube, as shown in Fig. 1. The HAp particles' size was in the 0.1 to 0.5 μm range, although aggregates with a diameter of approximately 1 to 2 μm were formed. The particle cohesion of the aggregates was modified with a ball mill prior to the experiments. An aerosol was produced by mixing the HAp particles with He gas using a vibration system. The processing chamber was pumped down with a mechanical booster pump and a rotary pump to produce a pressure difference between the two chambers. Helium gas flowed from the aerosol chamber to the processing chamber. The HAp particles were accelerated by the flow of helium gas and carried to the processing chamber through the Teflon tube and nozzle. The HAp particles ejected from the nozzle impacted with the substrate and were deposited on the substrate's surface. During the experiments the pressure difference between the two chambers was 1 atm. The nozzle employed in this experiment had a rectangular orifice of 6.0 x 0.3 mm in size.

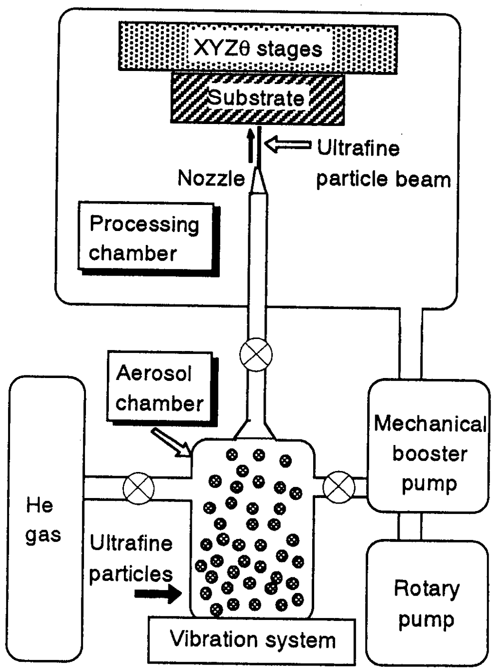

Fig. 1 Schematic configuration of the ultrafine particle beam processing and aerosol chambers.

The substrates were Ti plates polished to a roughness (Ra) of around 0.04 μm. The distance between the nozzle and the Ti plate was 10 mm. The incident angle of the UFP beam was varied from 0° to 60° with a period of 20° by rotation of the θ stage. The Ti plate's position was controlled with XYZ stages connected to a computer. An area of 6.0 x 5.0 mm on the surface of the Ti plate was scanned by the UFP beam for 1 min at room temperature. Neither the Ti plate nor the HAp particles were heated during the coating process.

The surfaces of the HAp films formed were examined with a scanning electron microscope (SEM) and the films' thicknesses were measured with a

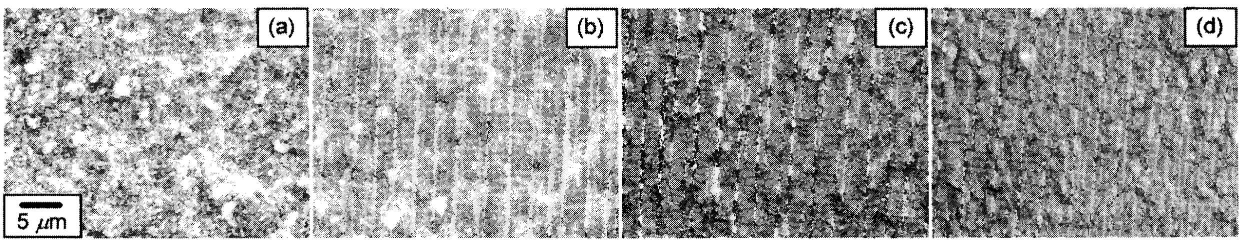

Fig. 2 HAp film surfaces observed with a scanning electron microscope at incident beam angles of (a) 0°, (b) 20°, (c) 40° and (d) 60°.

surface profiler. The adhesion strength was estimated using a tensile testing machine by attaching a brass rod with a diameter of 5 mm to the HAp film with epoxy resin. It was pulled with a loading rate of 0.2 mm/min until failure of the HAp film. The film's crystal structure was observed by X-ray diffraction (XRD).

3. Results and Discussion

The surfaces of the HAp films produced with the UFP beam at incident angles of 0°, 20°, 40° and 60° as observed with a SEM are shown in Figs. 2 (a), 2 (b), 2 (c) and 2 (d), respectively. As the images show, the roughness of the surface was modified as the incident angle increased. Measurement with a surface profiler also indicated that this modification was caused because Ra varied from 1.5 μm for an incident angle of 0° to 0.07 μm for 60°.

Figure 3 shows the thickness of the HAp film formed on the Ti plate as a function of the incident angle of the UFP beam. The thickness of the HAp film was a maximum (50 μm) for 0°, and decreased to 2.5 μm as the angle was increased to 60°. The HAp films formed at 0° and 20° were completely and partially broken, respectively, in a scratch test, which indicates that the HAp film formed at 0° had less cohesive strength and also less adhesion strength to the Ti plate than the film formed at 20°. Similarly, the film formed at 20° was weaker with regard to both cohesive strength and adhesion strength than those formed at 40° and 60°. In the tensile test of the films formed at 40° and 60°, the epoxy resin layer bonding the HAp film to the brass rod broke before the films failed. Although the absolute values could not be measured, the films' adhesion strength is assumed to be higher than 20 MPa, since the adhesion strength between the epoxy resin layer and brass rod was determined to be 20 MPa.

In the aerosol chamber in Fig. 1, there were particle aggregates with a diameter of 1 to 2 μm and dispersed submicron-size particles. The particle aggregates could also be accelerated by the gas flow and ejected from the nozzle. When they impacted with the Ti plate at an incident angle of 0°, they

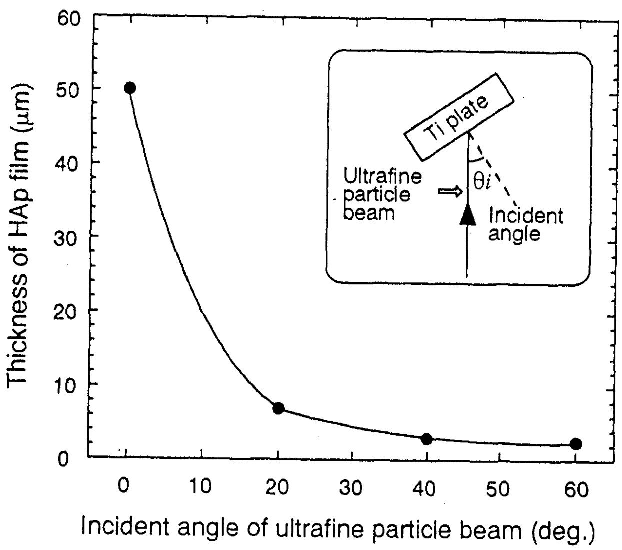

Fig. 3 Thickness of the HAp film formed on Ti plate as a function of the incident beam angle.

adhered to the substrate as Fig. 2 (a) suggests. However, the adhesion strength was low since the aggregate size was 1 to 2 μm. As described earlier, the adhesion mechanism is possibly the result of the localized thermal energy produced by submicron-size particles impacting at a speed of 200 - 650 m/s [8,9]. When particle aggregates impact other particle aggregates already deposited on the Ti plate, the bonding strength will be reduced. This could explain why the HAp film formed at 0° had low adhesion and cohesive strengths. Particle aggregates may also be deposited on the Ti plate at an oblique incidence as suggested in Fig. 2 (b), but in such a case a force is generated parallel to the surface in addition to the normal vector. This force acting parallel to the surface may push and remove particle aggregates with low adhesion that have been already deposited as more particles fly out from the nozzle. The mechanisms caused by oblique incidence thus prevent films with low adhesion from being formed on the Ti plate. Thus, at incident angles of 40° and 60°, particle aggregates were removed by the oblique incidence effect and fine HAp films with good adhesion were formed by the deposition of submicron-size particles.

The XRD patterns of the HAp particles used in this study and of the HAp film formed at 40° are shown in Figs. 4 (a) and (b). The crystallinity of HAp

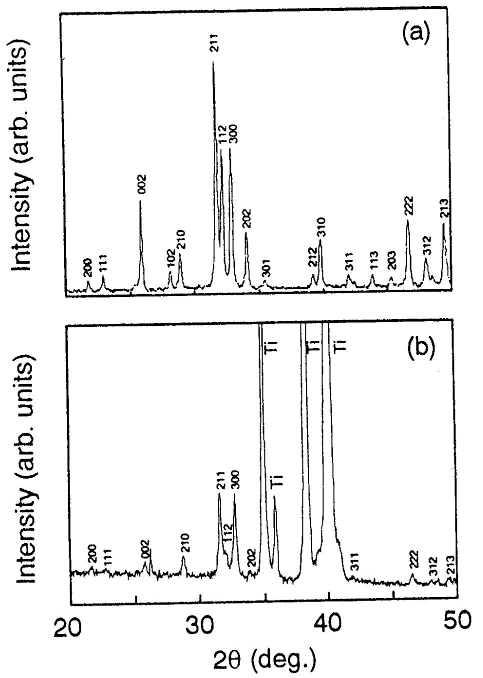

Fig. 4 X-ray diffraction pattern of (a) HAp powder and (b) the HAp film formed on Ti plate at an incident beam angle of 40°.

is retained throughout the process. The XRD patterns for 0°, 20° and 60° also indicate that the crystallinity was retained.

4. Conclusions

A HAp film fabrication system with the AD method utilizing a UFP beam was successfully developed. The thickness of the HAp film decreased as the incident angle increased. The HAp film's cohesive strength and adhesion strength were both improved by an oblique incidence effect. The HAp crystallinity was retained throughout the process.

References

1) K. deGroot, R. Geesink, C. P. A. T. Klein and P. Serekian: J. Biomed. Mater. Res. 21 (1987), p. 1375.
2) L. G. Ellies, L. C. Lucas, W. R. Lacefield and E. D. Rigney: Biomaterials 13 (1992) p. 313.
3) Y. C. Tsui, C. Doyle and T. W. Clyne: Biomaterials 19 (1998) p. 2015.
4) J. L. Ong and L. C. Lucas: Biomaterials 15 (1994) p. 337.
5) J.-M. Choi, H.-E. Kim and I.-S. Lee: Biomaterials 21 (2000) p. 469.
6) C. K. Wang, J. H. Chern Lin, C. P. Ju, H. C. Ong and R. P. H. Chang: Biomaterials 18 (1999) p. 1331
7) S. Kasyu, E. Fuchita, T. Manabe and C. Hayashi: Jpn. J. Appl. Phys. Part 2 23 (1984) p. L910.
8) M. Lebedev, J. Akedo, K. Mori and T. Eiji: J. Vac. Sci. & Technol. A 18 (2000) p. 563.
9) J. Akedo, M. Ichiki, K. Kikuchi and R. Maeda: Sens. & Actuat. A 69 (1998) p. 107.
10) R. C. Dykhuizen and M. F. Smith: J. Thermal Spray Technol. 7 (1998) p. 205.